

CONSTRAINING THE PROPERTIES OF SUPERMASSIVE BLACK HOLE SYSTEMS USING PULSAR TIMING: APPLICATION TO 3C 66B

FREDRICK A. JENET,¹ ANDREA LOMMEN,² SHANE L. LARSON,³ AND LINQING WEN⁴

Received 2003 October 10; accepted 2004 January 20

ABSTRACT

General expressions for the expected timing residuals induced by gravitational wave (G-wave) emission from a slowly evolving, eccentric, binary black hole system are derived here for the first time. These expressions are used to search for the signature of G-waves emitted by the proposed supermassive binary black hole system in 3C 66B. We use data from long-term timing observations of the radio pulsar PSR B1855+09. For the case of a circular orbit, the emitted G-waves should generate clearly detectable fluctuations in the pulse-arrival times of PSR B1855+09. Since no G-waves are detected, the waveforms are used in a Monte Carlo analysis in order to place limits on the mass and eccentricity of the proposed black hole system. The analysis presented here rules out the adopted system with 95% confidence. The reported analysis also demonstrates several interesting features of a G-wave detector based on pulsar timing.

Subject headings: black hole physics — gravitational waves — pulsars: general — pulsars: individual (B1855+09)

1. INTRODUCTION

This work describes a general technique used to constrain the properties of supermassive binary black hole (SBBH) systems using pulsar-timing observations. This technique is applied to the recently proposed SBBH system in 3C 66B (Sudou et al. 2003; hereafter S03) using 7 yr of timing data from the radio pulsar PSR B1855+09. Given the length of the available data set and this pulsar’s low rms timing noise (1.5 μ s), these data are well suited for this analysis.

Expressions are derived for the expected timing residuals induced by G-waves generated from two orbiting masses. The effects of orbital eccentricity, viewing geometry, and post-Newtonian orbital evolution are included. Since the resulting waveforms are quasi-periodic, although not necessarily sinusoidal, a periodogram analysis together with harmonic summing can be used to search for the signature of G-waves in pulsar-timing data. When this signature is detected, the derived expressions can be used to determine the system’s chirp mass and eccentricity. For a nondetection, these expression can be used in a Monte Carlo analysis in order to place limits on the properties of the proposed system.

In this work, the derived expressions are used to place limits on the proposed SBBH system in 3C 66B, a nearby ($z = 0.02$) radio galaxy. S03 recently suggested that this galaxy may contain a SBBH system with a current period of 1.05 yr, a total mass of $5.4 \times 10^{10} M_{\odot}$, and a mass ratio of 0.1. Such a system will merge in ~ 5 yr. Although it would be fortuitous to catch such a system so close to coalescence, the reward for directly detecting G-waves for the first time is large enough to warrant a short investigation focused on this system.

Future work will place constraints on other known nearby candidate SBBH systems. Lommen & Backer (2001) showed that meaningful constraints could be placed on about a dozen nearby sources, if pulsar timing can reach sensitivities of 100 ns. The residual expressions derived here can be used to place limits on the chirp mass and eccentricity of these systems. These expressions also show how the same G-wave will affect multiple sources, thus allowing one to discriminate between G-wave-induced and non-G-wave-induced timing fluctuations.

Section 2 describes the expected signature of G-wave emission from a general binary system; § 3 applies these results to the specific case of the proposed system in 3C 66B. The observations of PSR B1855+09 used to search for G-waves are described in § 4. Section 5 discusses the search techniques employed as well as the Monte Carlo simulation used to place limits on the mass and eccentricity of the system. The results are discussed in § 6.

2. THE SIGNATURE OF A SBBH

The orbital motion of a SBBH system will generate gravitational radiation. The emitted G-waves will induce periodic oscillations in the arrival times of individual pulses from radio pulsars. Given a model for the pulse arrival times in the absence of G-waves, one can generate a time series of “residuals,” which are the observed pulse arrival times minus the expected pulse arrival times. Ideally, the effects of known accelerations are removed from the timing residuals, leaving only the variations due to the presence of G-waves.

The emitted G-waves are described by two functions of spacetime, h_+ and h_{\times} , which correspond to the gravitational wave strain of the two polarization modes of the radiation field. As these waves pass between the Earth and a pulsar, the observed timing residuals, $R(t)$, will vary as (Estabrook & Wahlquist 1975; Detweiler 1979)

$$R(t) = \frac{1}{2} (1 + \cos \mu) [r_+(t) \cos(2\psi) + r_{\times}(t) \sin(2\psi)], \quad (1)$$

¹ California Institute of Technology, Jet Propulsion Laboratory, 4800 Oak Grove Drive, Pasadena, CA 91109.

² Franklin and Marshall College, Department of Physics and Astronomy, PO Box 3003, Lancaster, PA 17604.

³ California Institute of Technology, 1500 California Boulevard, Pasadena CA, 91125.

⁴ The LIGO Laboratory, California Institute of Technology, 1500 California Boulevard, Pasadena, CA 91125.

where t is time, μ is the opening angle between the G-wave source and the pulsar relative to Earth, ψ is the G-wave polarization angle, and the “+” and “ \times ” refer to the two G-wave polarization states. The functions r_+ and r_\times , referred to collectively as $r_{+\times}$, are related to the G-wave strain by

$$r_{+\times}(t) = r_{+\times}^e(t) - r_{+\times}^p(t), \quad (2)$$

$$r_{+\times}^e(t) = \int_0^t h_{+\times}^e(\tau) d\tau, \quad (3)$$

$$r_{+\times}^p(t) = \int_0^t h_{+\times}^p \left[\tau - \frac{d}{c} (1 - \cos \mu) \right] d\tau, \quad (4)$$

where $h_{+\times}^e(t)$ is the G-wave strain at Earth, $h_{+\times}^p(t)$ is the gravitational wave strain at the pulsar, τ is the time integration variable, d is the distance between Earth and the pulsar, and c is the speed of light. Note that the pulsar term, $h_{+\times}^p$, is evaluated at the current time minus a geometric delay.

G-waves emitted by a system in a circular orbit (i.e., zero eccentricity) will vary sinusoidally as a function of time, with a frequency given by twice the orbital frequency. For eccentric systems, the emitted waves will contain several harmonics of the orbital frequency. The second harmonic will dominate at low eccentricities, while the fundamental (i.e., the orbital) frequency will dominate at high eccentricities. In general, the period and eccentricity of a binary system will be decreasing with time, because the system is radiating away energy and angular momentum in G-waves. Hence, the frequencies present in $h_{+\times}(t)$ will vary with time. Since $r_{+\times}^e$ and $r_{+\times}^p$ may be generated by $h_{+\times}(t)$ at epochs separated by an extremely long time interval, the frequency content of these terms may differ significantly.

The G-wave strain, $h(t)$, induced by a black hole binary can be calculated using the standard weak-field approximation applied to two orbiting point masses (Wahlquist 1987). The expected residuals are found by integrating $h(t)$ with respect to time (see eqs. [2]–[4]):

$$r_+^e(t) = \alpha(t) [A(t) \cos(2\phi) - B(t) \sin(2\phi)], \quad (5)$$

$$r_\times^e(t) = \alpha(t) [A(t) \sin(2\phi) + B(t) \cos(2\phi)], \quad (6)$$

$$\alpha(t) = \frac{M_c^{5/3}}{D\omega^{1/3}} \frac{\sqrt{1-e(t)^2}}{1+e(t)\cos[\theta(t)]}, \quad (7)$$

where D is the distance to the source, ϕ is the orientation of the line of nodes on the sky, $\omega(t)$ is the orbital frequency, $e(t)$ is the eccentricity, $\theta(t)$ is the orbital phase, and M_c is the “chirp mass,” defined as

$$M_c = M_t \left(\frac{m_1 m_2}{M_t^2} \right)^{3/5}, \quad (8)$$

where $M_t = m_1 + m_2$ and m_1 and m_2 are the masses of the individual black holes. Note that all units from equation (5) on are in “geometrized” units,⁵ where $G = c = 1$. $A(t)$ and $B(t)$ are given by

$$A(t) = 2e(t) \sin[\theta(t)] \left\{ \cos[\theta(t) - \theta_n]^2 - \cos[i]^2 \sin[\theta(t) - \theta_n]^2 \right\} - \frac{1}{2} \sin\{2[\theta(t) - \theta_n]\} \{1 + e(t) \cos[\theta(t)]\} [3 + \cos(2i)], \quad (9)$$

$$B(t) = 2 \cos i (\cos\{2[\theta(t) - \theta_n]\} + e(t) \cos[\theta(t) - 2\theta_n]), \quad (10)$$

where i and θ_n are the orbital inclination angle and the value of θ at the line of nodes, respectively (Wahlquist 1987). Values for $\theta(t)$ and $e(t)$ are given by the coupled differential equations (Wahlquist 1987; Peters 1964)

$$\frac{d\theta}{dt} = \omega(t) \frac{\{1 + e(t) \cos[\theta(t)]\}^2}{[1 - e(t)^2]^{3/2}}, \quad (11)$$

$$\frac{de}{dt} = -\frac{304}{15} M_c^{5/3} \omega_0^{8/3} \chi_0^{-4} \frac{e(t)^{-29/19} [1 - e(t)^2]^{3/2}}{[1 + (121/304)e(t)^2]^{1181/2299}}, \quad (12)$$

where ω_0 is the initial value of $\omega(t)$ and χ_0 is a constant that depends on the initial eccentricity e_0 :

$$\chi_0 = (1 - e_0^2) e_0^{-12/19} \left[1 + \frac{121}{304} e_0^2 \right]^{-870/2299}. \quad (13)$$

Here $\omega(t)$ is given by

$$\omega(t) = a_0 e(t)^{-18/19} [1 - e(t)^2]^{3/2} \left[1 + \frac{121}{304} e(t)^2 \right]^{-1305/2299}, \quad (14)$$

where a_0 is determined by the initial condition $\omega(t=0) = \omega_0$. The above equations are accurate to first order in v/c and valid only when both $e(t)$ and $\omega(t)$ vary slowly with time. The expressions for $r_{+\times}^p$ are identical to those for $r_{+\times}^e$. Note that $r_{+\times}^p$ is evaluated at an earlier time than $r_{+\times}^e$ (see eqs. [3] and [4]).

3. APPLICATION TO 3C 66B

S03 suggest the presence of a $1.3 \times 10^{10} M_\odot$ black hole binary in the radio galaxy 3C 66B. Their VLBI measurements at both 8.4 and 2.3 GHz show the elliptical motion of a radio core with a period of 1.05 ± 0.03 yr at epoch 2002. Normally, this motion would be attributed to the precession of a jet (e.g., Katz 1997), but in this case, S03 argue that the observed motion is due to the orbit of the jet’s source, a supermassive black hole, around a supermassive black hole companion. Concerning these claims, we note several issues. First, only a single orbit is observed, i.e., the elliptical motion has not yet been shown to be repeatable. Second, S03 do not address the possibility that the observed elliptical motion, which is perilously close to having a 1 yr period, is somehow the result of the Earth’s motion around the Sun. Third, they suggest that the system will merge in about 5 yr. Hence, the a priori probability that we have “caught” such a system in the act of coalescence is very low. Nonetheless, the proposed system would generate

⁵ In geometrized units, mass and distance are in units of time.

G-waves detectable in currently available pulsar-timing data, and we can independently and observationally verify or refute this claim. Given the huge payoff for detecting G-waves for the first time, it is worth an analysis of existing data. In this section we show how G-waves from the S03 system would affect the timing residuals of PSR B1855+09, and in §§ 4 and 5 we show that there are no detectable G-waves from this system in the timing data. Consequently, limits are placed on the properties of the system.

Using the SBBH parameters adopted by S03, the expressions derived in § 2 can be used to determine the expected timing residuals. The angle between 3C 66B and PSR B1855+09 on the sky is 81.5° , and PSR B1855+09 lies 1 ± 0.3 kpc away (Kaspi, Taylor, & Ryba 1994; hereafter KTR94). The total time delay between the pulsar epoch and the Earth epoch, $(d/c)(1 - \cos \mu)$, is 3700 ± 1100 yr (see eq. [4]). Since the time delay between the Earth and the pulsar is much larger than the timescale for evolution of the system, the expected residual will contain a low-frequency component due to the pulsar term ($r_{+,x}^p$) and a high-frequency component due to the Earth term ($r_{+,x}^e$). This effect is referred to as the “two-frequency” response and is analogous to the three-pulse response occurring in spacecraft Doppler-tracking experiments (Estabrook & Wahlquist 1975) and the multi-pulse response from time-delay interferometry used in the proposed *Laser Interferometer Space Antenna* (LISA) mission (Armstrong, Estabrook, & Tinto 1999). The top panel in Figure 1 shows a theoretical set of timing residuals due to G-wave emission from the proposed binary system in 3C 66B, assuming that the distance to this galaxy is 80 Mpc and the distance to the pulsar is 1 kpc. This waveform was generated with $i = \theta_n = \phi = 0$ and $\psi = \pi/4$. The chirp mass used was $1.3 \times 10^{10} M_\odot$, and the orbital period at the epoch of the S03 observations (i.e., MJD = 51981) was taken to be 1.05 yr. The eccentricity at this epoch was taken to be 0.0001. Two distinct oscillation frequencies can be seen, one with a period of about 0.88 yr and the other with a period around 6.24 yr. The bottom panel in Figure 1 shows the Lomb periodogram (see § 4) of the simulated residuals. In general, the orbital geometry and eccentricity of this system is unknown. Fortunately, the expected signature will be periodic regardless of these parameters. Hence, one can search for the signature

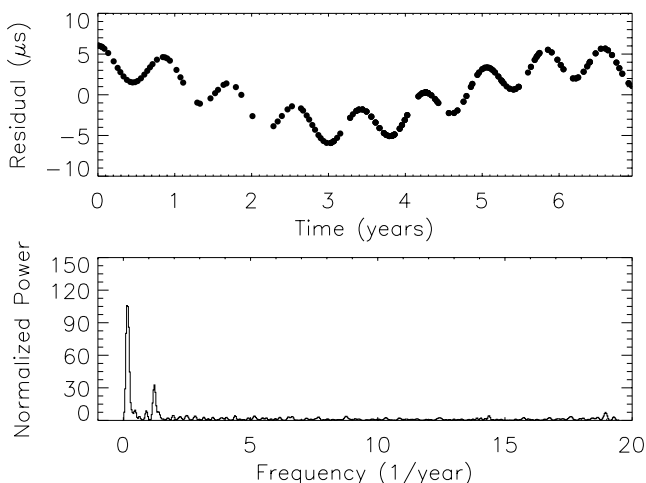


FIG. 1.—*Top*: Theoretical timing residuals induced by G-waves from 3C 66B. The timing points are chosen to coincide with the actual timing residuals of PSR B1855+09. *Bottom*: The corresponding normalized Lomb periodogram.

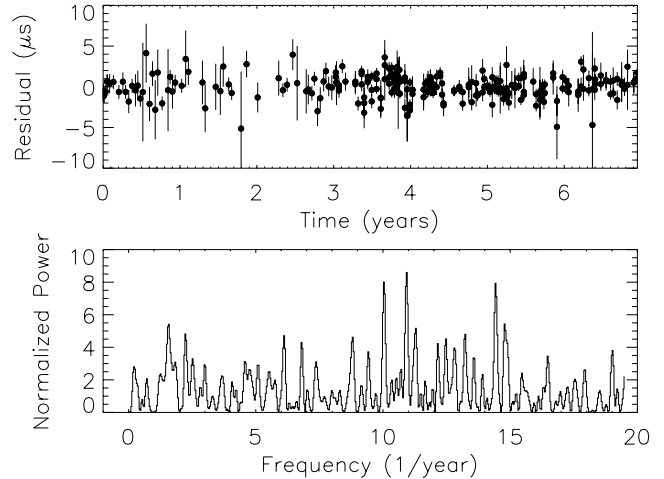


FIG. 2.—*Top*: Timing residuals for PSR B1855+09. *Bottom*: The corresponding normalized Lomb periodogram.

of G-waves using periodogram techniques together with harmonic summing.

4. TIMING OBSERVATIONS OF PSR B1855+09

We used observations of PSR B1855+09 made by KTR94 at the Arecibo Observatory 300 m telescope⁶ and made public therein. The KTR94 data set is made up of more than 7 yr (1986–1993) of biweekly observations using the Princeton University MarkIV system. For details on data acquisition, reduction, and clock correction, please see KTR94.

The times of arrival were fit to the model published by KTR94 using the standard TEMPO software package.⁷ We used their best-fit values as our initial parameters. In the fitting, we allowed the spin period (P), period derivative (\dot{P}), right ascension, declination, proper motion, parallax, and the five Keplerian binary parameters to vary. Additionally, the Shapiro delay parameters were included in the model but were fixed at the optimum values published by KTR94. The best-fit values of all parameters were consistent with those published by KTR94. The resulting timing residuals used are shown in the top panel of Figure 2.

5. CONSTRAINTS FROM PULSAR TIMING

The timing residuals from PSR B1855+09 were searched for the signature of G-waves, using the normalized Lomb periodogram (LP; see Press et al. 1992, § 13.8) together with “harmonic summing.” The LP is the analog of the discrete Fourier transform for unevenly sampled data. Harmonic summing is performed by adding together the periodogram power at harmonics of each frequency up to a chosen maximum harmonic (Lyne 1989). This process increases the sensitivity to periodic, nonsinusoidal waveforms such as those expected from eccentric binaries. If a SBBH system existed in 3C 66B with an eccentricity of zero and with the chirp mass and period adopted by S03, then the LP should show the two-frequency response like that seen in Figure 1. Figure 2 plots the normalized LP for the residual data described above. The periodogram power was calculated for 542 frequencies

⁶ The National Astronomy and Ionosphere Center Arecibo Observatory is operated by Cornell University under contract with the National Science Foundation.

⁷ See <http://pulsar.princeton.edu/tempo>.

ranging from $1/27.8 \text{ yr}^{-1}$ to 19.5 yr^{-1} , with a resolution of $1/27.8 \text{ yr}^{-1}$. This corresponds to a frequency-oversampling factor of 4. There are no significant peaks in this LP. For the purposes of this paper, a significant peak has less than a 0.1% chance of occurring in purely random data assuming Gaussian statistics. Harmonic summing was performed up to the sixth harmonic. Again, no significant features were found.

Since the LP analysis was unable to detect the presence of G-waves in the timing residuals, limits can be placed on the possible chirp mass and eccentricity of the system. Since the general waveform given by equations (5)–(7) depends on various unknown quantities that specify the orientation of the orbit and the viewing geometry, a Monte Carlo simulation was performed in order to determine the probability of detecting a SBBH system in 3C 66B with a given chirp mass and eccentricity. Aside from M_c and e , the general waveform depends on six angles: two angles specify the plane of the orbit, two determine the orbital phase of binary at the beginning of each of the two relevant epochs, and two determine the initial location of the line of nodes at the start of each epoch. For a given M_c and e , the initial eccentricities and periods were determined using equations (11) and (12). An orbital period of 1.05 yr at MJD = 51981 was chosen for the initial parameters in order to match the observations of S03. The distances to 3C 66B and PSR B1855+09 were taken to be 80 Mpc and 1 kpc, respectively. The six unknown angles were chosen at random from a uniform distribution that ranged from 0 to 2π , and a corresponding waveform was generated using equations (5)–(14). The waveform was then added to the residual data. When processing the timing data, the program TEMPO will remove the effects of the Earth's orbit and parallax together with a linear trend. In order to simulate the effects of removing these components from the data, various functions were subtracted from the simulated data. A 1 yr periodicity was removed by subtracting a function of the form $y = a \cos(\omega t) + b \sin(\omega t)$ where t is time, $\omega = 2\pi/1 \text{ yr}$, and a and b are determined by a least-squares fit to the simulated data. A 6 month periodicity was removed in a similar fashion. A best-fit first-order polynomial was also removed. This combination of data plus simulated signal minus various fitted functions was then analyzed using the LP method described above. If a significant peak was found (see above), then the signal was considered to be detected. A total of 1000 waveforms were tested for each M_c and initial e . It was found that there is a 98% chance of detecting a system like that adopted by S03, if it has an eccentricity less than 0.03. As the eccentricity increases above 0.03, the system is evolving rapidly enough to make the period at the earlier epoch (i.e., the period in the pulsar term), much longer than the observation length. Hence, for eccentricities between 0.03 and 0.49, the probability drops to about 95%. The detection probability starts falling off again above eccentricities of 0.49. At this point, the period of the binary system at the start of the observations is longer than the observing time. The results for this and other chirp masses are summarized in Table 1. The first column lists the chirp mass in $10^{10} M_\odot$, the next four columns list the limiting eccentricities at the 98%, 95%, and 90% probability levels. For example, with $M_c = 1.0$, if the eccentricity at the epoch of the S03 observations was less than 0.03, then there was at least a 95% chance of detecting the system.

6. DISCUSSION

The signature of G-waves emitted by the proposed system in 3C 66B was not found in the analysis of the pulsar-timing residuals of PSR B1855+09. The system adopted by

TABLE 1
DETECTION LIMITS

M_c ($10^{10} M_\odot$)	MAXIMUM ECCENTRICITY		
	98%	95%	90%
1.3.....	0.03	0.49	0.51
1.2.....	0.02	0.49	0.51
1.1.....	0.02	0.16	0.23
1.0.....	...	0.03	0.18
0.9.....	...	0.02	0.04
0.8.....	...	0.01	0.03
0.7.....

NOTE.—Maximum eccentricity given a chirp mass, M_c , for the proposed system at the epoch of the S03 observations for 98%, 95% and 90% minimum detection probabilities. The ellipses mean that the probability of detecting the system never reached the specified value.

S03 has a total mass of $5.4 \times 10^{10} M_\odot$ and a chirp mass of $1.3 \times 10^{10} M_\odot$. The confidence with which such a system can be ruled out depends on its eccentricity, which is not constrained by the S03 observations. It is generally accepted that the eccentricity of a system near coalescence will be small, but exactly how small depends on many unknown aspects of the system's formation and evolution. If the eccentricity is less than 0.03, then the adopted system may be ruled out at the 98% confidence level. As the assumed eccentricity of the system increases, its expected lifetime will decrease. Given that the system had to exist for longer than 1 yr and assuming that it will merge when it reaches the last stable orbit, it can be shown that the eccentricity must be less than 0.3 for a black hole binary system with negligible spins. In this case, the system can be ruled out at the 95% confidence level.

Even though the pulsar data show that the adopted system is highly unlikely, it is possible that the system has a lower chirp mass. $M_c < 0.7 \times 10^{10} M_\odot$ cannot be ruled out regardless of e . For the case of $e = 0$, a lower bound of 12 yr can be placed on the lifetime of the system. Systems with $M_c = 1.0 \times 10^{10}$ and $0.8 \times 10^{10} M_\odot$ are allowable when e is larger than 0.18 and 0.03, respectively.

The above discussion assumed a value of $75 \text{ km s}^{-1} \text{ Mpc}^{-1}$ for the Hubble constant when calculating the distance to 3C 66B. For other values, the chirp masses listed in Table 1 need to be multiplied by a factor of $(H/75)^{-3/5}$, where H is the desired Hubble constant in units of $\text{km s}^{-1} \text{ Mpc}^{-1}$. For Hubble constants within the range of 65 to $85 \text{ km s}^{-1} \text{ Mpc}^{-1}$, the chirp masses listed in Table 1 are valid to within 10%.

This analysis can be applied to any SBBH candidate, the list of which is growing. It is generally accepted that most galaxies, both active (Wandel 1999; Kaspi et al. 2000; Ferrarese et al. 2001; Merritt & Ferrarese 2001) and nonactive (Richstone et al. 1998; Ferrarese & Merritt 2000; Gebhardt et al. 2000; Tremaine et al. 2002) contain supermassive black holes. The current debate centers on how best to measure their masses. The range of masses, however, is not debated. For active galaxies, Ferrarese et al. (2001) use stellar velocity dispersions to substantiate the masses found via reverberation mapping (Kaspi et al. 2000; Wandel 1999). These authors find about three dozen massive black holes with masses up to $5.5 \times 10^8 M_\odot$. However, none of these are closer than 3C 66B. For nonactive galaxies, Ferrarese et al. (2001), Merritt & Ferrarese

(2001), and Tremaine et al. (2002) debate the relationship between the velocity dispersion and the mass, but between them they are working with a collection of about three dozen galaxies whose central black holes have been estimated to have masses of more than $2.5 \times 10^9 M_{\odot}$, two-thirds of which are closer than 20 Mpc. All of the above black holes may actually be binary systems. Future pulsar timing work will be able to constrain the chirp mass of these sources and hence limit the mass of the possible binary companions.

Pulsar timing is becoming more sensitive (e.g., van Straten et al. 2001) and more millisecond pulsars are being found (e.g., McLaughlin et al. 2003), some of which may have lower noise characteristics than PSR B1855+09, the source used in this study. The residual waveforms presented here will be

useful in searching such high-quality data for the signatures of SBBH systems.

Part of this research was carried out at the Jet Propulsion Laboratory, California Institute of Technology, under a contract with the National Aeronautics and Space Administration and funded through the internal Research and Technology Development program. A. L. acknowledges support of NSF grant 0107342. L. W. acknowledges support of the LIGO Laboratory at Caltech and NSF grants PHY-0071050 and PHY-0107417. The authors wish to thank John Armstrong and Michael Eracleous for useful discussions.

REFERENCES

- Armstrong, J. A., Estabrook, F. B., & Tinto, M. 1999, *ApJ*, 527, 814
 Detweiler, S. 1979, *ApJ*, 234, 1100
 Estabrook, F. B., & Wahlquist, H. D. 1975, *Gen. Relativ. Gravitation*, 6, 439
 Ferrarese, L., & Merritt, D. 2000, *ApJ*, 539, L9
 Ferrarese, L., Pogge, R. W., Peterson, B. M., Merritt, D., Wandel, A., & Joseph, C. L. 2001, *ApJ*, 555, L79
 Gebhardt, K., et al. 2000, *ApJ*, 539, L13
 Kaspi, S., Smith, P. S., Netzer, H., Maoz, D., Jannuzi, B. T., & Giveon, U. 2000, *ApJ*, 533, 631 (KTR94)
 Kaspi, V. M., Taylor, J. H., & Ryba, M. F. 1994, *ApJ*, 428, 713
 Katz, J. I. 1997, *ApJ*, 478, 527
 Lommen, A. N., & Backer, D. C. 2001, *ApJ*, 562, 297
 Lyne, A. G. 1989, in *Gravitational Wave Data Analysis*, ed. B. F. Schutz (NATO ASI Series C, 253; Dordrecht: Kluwer), 95
 McLaughlin, M. A., Lorimer, D. R., Arzoumanian, Z., Backer, D. C., Cordes, J. M., Fruchter, A. S., Lommen, A. N., & Xilouris, K. 2003, in *IAU Symp. 218, Young Neutron Stars and their Environment*, ed. F. Camilo & B. M. Gaensler (San Francisco: ASP), 220
 Merritt, D., & Ferrarese, L. 2001, *MNRAS*, 320, L30
 Peters, P. C., 1964, *Phys. Rev.*, 136, 1224
 Press, W. H., Teukolsky, S. A., Vetterling, W. T., & Flannery, B. P. 1992, *Numerical Recipes in C: The Art of Scientific Computing* (2nd Ed.; Cambridge: Cambridge Univ. Press)
 Richstone, D., et al. 1998, *Nature*, 395, A14
 Sudou, H., Iguchi, S., Murata, Y., & Taniguchi, Y. 2003, *Science*, 300, 1263 (SO3)
 Tremaine, S., et al. 2002, *ApJ*, 574, 740
 van Straten, W., Bailes, M., Britton, M., Kulkarni, S. R., Anderson, S. B., Manchester, R. N., & Sarkissian, J. 2001, *Nature*, 412, 158
 Wahlquist, H. 1987, *Gen. Relativ. Gravitation*, 19, 1101
 Wandel, A. 1999, *ApJ*, 519, L39